

## Anisotropic small-polaron hopping in W:BiVO<sub>4</sub> single crystals

Alexander J. E. Rettie, William D. Chemelewski, Jeffrey Lindemuth, John S. McCloy, Luke G. Marshall, Jianshi Zhou, David Emin, and C. Buddie Mullins

Citation: *Applied Physics Letters* **106**, 022106 (2015); doi: 10.1063/1.4905786

View online: <http://dx.doi.org/10.1063/1.4905786>

View Table of Contents: <http://scitation.aip.org/content/aip/journal/apl/106/2?ver=pdfcov>

Published by the *AIP Publishing*

---

### Articles you may be interested in

[Electrochromism and small-polaron hopping in oxygen deficient and lithium intercalated amorphous tungsten oxide films](#)

*J. Appl. Phys.* **118**, 024901 (2015); 10.1063/1.4926488

[Nature of small-polaron hopping conduction and the effect of Cr doping on the transport properties of rare-earth manganite La<sub>0.5</sub>Pb<sub>0.5</sub>Mn<sub>1-x</sub>Cr<sub>x</sub>O<sub>3</sub>](#)

*J. Chem. Phys.* **115**, 1550 (2001); 10.1063/1.1378018

[Polaron hopping conduction and thermoelectric power in LaMnO<sub>3+δ</sub>](#)

*J. Appl. Phys.* **89**, 4955 (2001); 10.1063/1.1362411

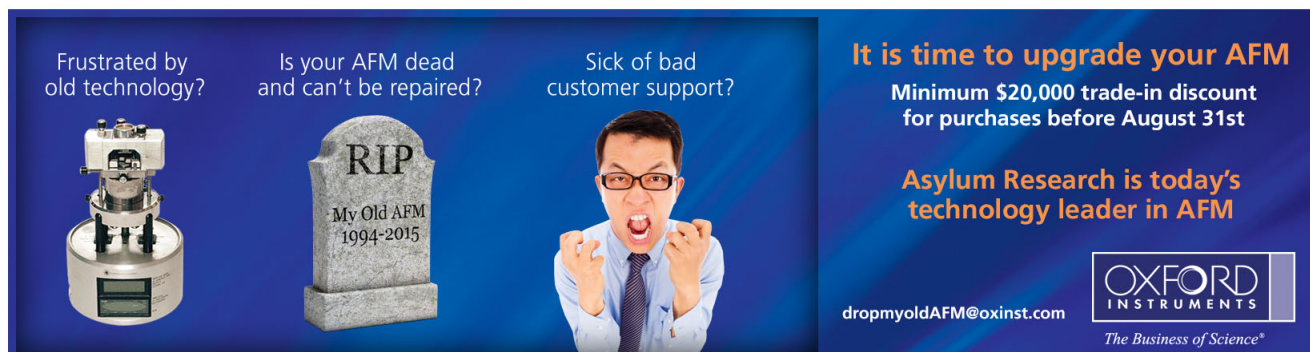
[Small polaron and bipolaron transport in antimony oxide doped barium hexaferrites](#)

*J. Appl. Phys.* **88**, 6526 (2000); 10.1063/1.1309045

[Multiphonon hopping conduction in nonconventional chromium-doped Bi<sub>3</sub>Pb<sub>1</sub>Sr<sub>3</sub>Ca<sub>3</sub>Cu<sub>4-n</sub>Cr<sub>n</sub>O<sub>x</sub> \(n=0.025–0.2\) glasses with nanocrystalline particles and clusters](#)

*J. Appl. Phys.* **88**, 5033 (2000); 10.1063/1.1317237

---

The advertisement features a dark blue background with three panels. The first panel shows an AFM with the text 'Frustrated by old technology?'. The second panel shows a tombstone with 'RIP My Old AFM 1994-2015' and the text 'Is your AFM dead and can't be repaired?'. The third panel shows a man shouting with the text 'Sick of bad customer support?'. To the right, a large text block reads 'It is time to upgrade your AFM' followed by 'Minimum \$20,000 trade-in discount for purchases before August 31st'. Below this is 'Asylum Research is today's technology leader in AFM'. At the bottom right is the Oxford Instruments logo with the tagline 'The Business of Science®' and the email 'dropmyoldAFM@oxinst.com'.

## Anisotropic small-polaron hopping in W:BiVO<sub>4</sub> single crystals

Alexander J. E. Rettie,<sup>1</sup> William D. Chemelewski,<sup>2</sup> Jeffrey Lindemuth,<sup>3</sup> John S. McCloy,<sup>4,5</sup> Luke G. Marshall,<sup>2,6</sup> Jianshi Zhou,<sup>2</sup> David Emin,<sup>7</sup> and C. Buddie Mullins<sup>1,2,8,a)</sup>

<sup>1</sup>McKetta Department of Chemical Engineering, The University of Texas at Austin, Austin, Texas 78712, USA

<sup>2</sup>Texas Materials Institute, The University of Texas at Austin, Austin, Texas 78712, USA

<sup>3</sup>Lake Shore Cryotronics, Westerville, Ohio 43081, USA

<sup>4</sup>School of Mechanical and Materials Engineering, Washington State University, Pullman, Washington 99164, USA

<sup>5</sup>Materials Science and Engineering Program, Washington State University, Pullman, Washington 99164, USA

<sup>6</sup>Department of Chemical Engineering, Northeastern University, Boston, Massachusetts 02115, USA

<sup>7</sup>Department of Physics and Astronomy, The University of New Mexico, Albuquerque, New Mexico 87131, USA

<sup>8</sup>Department of Chemistry, The University of Texas at Austin, Austin, Texas 78712, USA

(Received 24 November 2014; accepted 30 December 2014; published online 12 January 2015)

DC electrical conductivity, Seebeck and Hall coefficients are measured between 300 and 450 K on single crystals of monoclinic bismuth vanadate that are doped *n*-type with 0.3% tungsten donors (W:BiVO<sub>4</sub>). Strongly activated small-polaron hopping is implied by the activation energies of the Arrhenius conductivities (about 300 meV) greatly exceeding the energies characterizing the falls of the Seebeck coefficients' magnitudes with increasing temperature (about 50 meV). Small-polaron hopping is further evidenced by the measured Hall mobility in the *ab*-plane ( $10^{-1} \text{ cm}^2 \text{ V}^{-1} \text{ s}^{-1}$  at 300 K) being larger and much less strongly activated than the deduced drift mobility (about  $5 \times 10^{-5} \text{ cm}^2 \text{ V}^{-1} \text{ s}^{-1}$  at 300 K). The conductivity and *n*-type Seebeck coefficient is found to be anisotropic with the conductivity larger and the Seebeck coefficient's magnitude smaller and less temperature dependent for motion within the *ab*-plane than that in the *c*-direction. These anisotropies are addressed by considering highly anisotropic next-nearest-neighbor ( $\approx 5 \text{ \AA}$ ) transfers in addition to the somewhat shorter ( $\approx 4 \text{ \AA}$ ), nearly isotropic nearest-neighbor transfers. © 2015 AIP Publishing LLC. [<http://dx.doi.org/10.1063/1.4905786>]

Monoclinic bismuth vanadate (BiVO<sub>4</sub> or BVO) is a promising photo-anode for solar water splitting because (1) its band edges are well positioned for water oxidation, (2) its band gap is modest,  $\sim 2.5 \text{ eV}$ , and (3) it is stable in aqueous environments when coupled with co-catalysts.<sup>1–3</sup> However, the low electrical conductivity of BVO limits its utility as a photo-electrode.<sup>4–6</sup> This low conductivity was preliminarily ascribed to its charge carriers forming small polarons and a low temperature-independent Hall mobility.<sup>4</sup>

Small polarons can form when electronic charge carriers move slowly enough to displace surrounding atoms from their equilibrium positions.<sup>7</sup> Thus, small polarons are found in non-crystalline solids<sup>8–10</sup> as well as in well-ordered transition-metal<sup>11–14</sup> and organic<sup>15–17</sup> compounds, where slow electronic motion is attributed to disorder and to narrow electronic energy bands, respectively.

Here, we report measurements of the dc conductivity, Seebeck and Hall coefficients of *n*-type tungsten-doped BVO single crystals from 300 to 450 K. Detailed analysis of the anisotropic transport of W:BVO finds it consistent with adiabatic small-polaron hopping. Furthermore, we demonstrate that the anisotropy of transport is plausibly linked to structural differences in the arrangement of V ions.

The synthesis of single crystal samples of BVO with 0.3% W has been described in detail previously.<sup>4</sup> Four point

collinear conductivity and AC field Hall effect were conducted at Lake Shore Cryotronics on an 8404 AC/DC Hall measurement system. Measurement of the Seebeck coefficient was performed using a laboratory-built apparatus at UT Austin. Experimental details, calculation of geometrical factors, and a full description of the data analysis are provided in the supplemental material.<sup>18</sup>

The unit cell of monoclinic BVO is only slightly distorted from that for a tetragonal structure (where  $a = b$ ). Thus, we describe the transport as that for a tetragonal structure, only differentiating between transport in the *ab*-plane (perpendicular to the *c*-axis) and that along the *c*-axis.

The electrical conductivities ( $\sigma$ ) measured in the *ab*-plane and parallel to the *c*-axis are plotted versus temperature in Fig. 1(a). These measurements agree with our previous work.<sup>4</sup> The anisotropy ratio of the conductivity  $\sigma_{ab}/\sigma_c = 2.3 \pm 0.4$  is constant over the temperature range of 300–450 K. As shown in Fig. 1(b), these data can be described with the formula

$$\sigma(T) = \sigma_0(T) \exp\left(-\frac{E_\sigma}{\kappa T}\right), \quad (1)$$

with the pre-exponential factor  $\sigma_0(T) \propto 1/T$ , where  $E_\sigma$  is the conductivity activation energy,  $\kappa$  is the Boltzmann constant, and  $T$  is the absolute temperature. The first two columns of Table I list the activation energies and pre-exponential factors at 300 K for transport in the *ab*-plane and in the *c*-direction.

<sup>a)</sup> Author to whom correspondence should be addressed. Electronic mail: mullins@che.utexas.edu

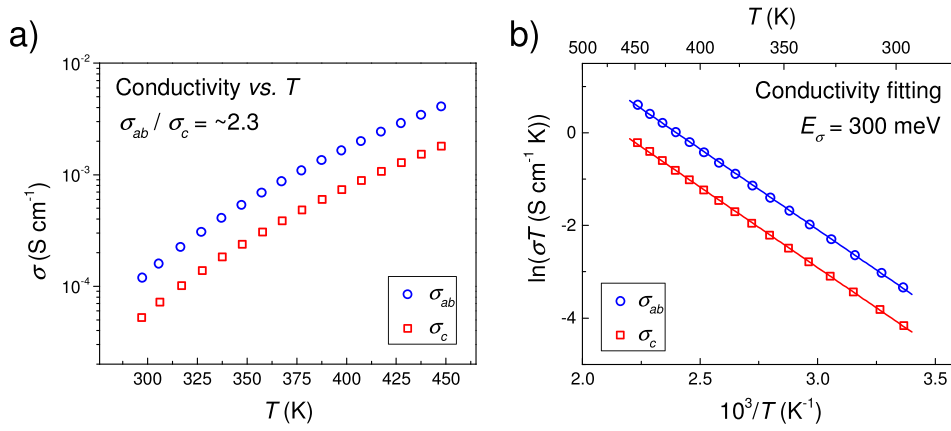


FIG. 1. The dc electrical conductivities in the  $ab$ -plane and parallel to the  $c$ -axis are plotted versus temperature in (a). The solid lines in (b) show the data's fit to Eq. (1).

TABLE I. Conductivity and Seebeck coefficient fitting parameters.

	$E_\sigma$ (meV)	$\sigma_0$ (S cm $^{-1}$ ) at 300 K	$E_S$ (meV)	$A$ (dimensionless)
$ab$ -plane	$300 \pm 1$	$14.2 \pm 0.4$	$47 \pm 4$	$4.3 \pm 0.1$
$c$ -axis	$300 \pm 1$	$6.1 \pm 0.2$	$83 \pm 3$	$5.2 \pm 0.1$

The Seebeck coefficients are plotted versus  $10^3/T$  in Fig. 2. This data has been fit to

$$S = -\frac{\kappa}{e} \left( \frac{E_S}{\kappa T} + A \right), \quad (2)$$

where  $e$  is the magnitude of an electron's charge,  $E_S$  is the Seebeck coefficient's characteristic energy, and  $A$  is a dimensionless constant.<sup>7,10</sup> The third and fourth columns of Table I list these fitting parameters. Significantly, the characteristic Seebeck energies are much smaller than  $E_\sigma$  (300 meV). These energy differences indicate that the activated conductivity is produced by carriers' thermally assisted hopping rather than from trap-modulated transport.<sup>7,19</sup>

The Hall mobility in the  $ab$ -plane is the product of the Hall constant  $R_{Hall}$  measured with the magnetic field parallel to the  $c$ -axis and the electrical conductivity in the  $ab$ -plane,  $\mu_{Hall} \equiv \sigma_{ab} R_{Hall}$ . The Hall mobility in the  $ab$ -plane is plotted

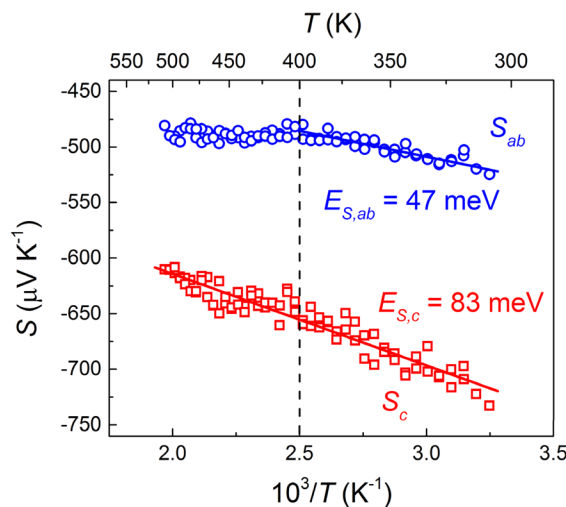


FIG. 2. Seebeck coefficients measured in the  $ab$ -plane and along the  $c$ -axis are plotted versus reciprocal temperature. Fits to Eq. (2) are shown with solid lines. The dashed vertical line at 400 K highlights a change of slope.

against reciprocal temperature in Fig. 3. For comparison, we also plot the drift mobility in the  $ab$ -plane deduced from measurements of the conductivity and Seebeck coefficients in the  $ab$ -plane,  $\mu_{d,ab} \propto \exp[-(E_\sigma - E_{s,ab})/\kappa T]$ , where we have chosen the intercept at  $1/T=0$  to be  $1 \text{ cm}^2 \text{ V}^{-1} \text{ s}^{-1}$ . This assumption is consistent with small-polaron hopping in the adiabatic regime, whose validity will be demonstrated in the following analysis.

BVO adopts a monoclinic scheelite structure at ambient conditions (space group  $I2/b$ ,  $a = 5.1935 \text{ \AA}$ ,  $b = 5.0898 \text{ \AA}$ ,  $c = 11.6972 \text{ \AA}$ , and  $\gamma = 90.387^\circ$ , Fig. 4(a)).<sup>20</sup> Although dopants can alter the lattice parameters, the changes are negligible at the dopant concentrations considered here.<sup>21</sup> The conduction band of BVO is of primarily V 3d character while the valence band is made up of O 2p and Bi 6s states.<sup>22</sup> W dopants substitute for V atoms and act as electron donors.<sup>4</sup> Excess electrons in BVO have been predicted to favorably localize on vanadium atoms,<sup>23</sup> thus we presume hopping to occur between the V sites.

Let us consider the physical origin of the transport anisotropy in W:BVO (Figs. 1 and 2). Nearest-neighbor (NN) jumps can be viewed as proceeding along zig-zag chains in the  $a$ - $c$  and  $b$ - $c$  directions with jump lengths of  $3.8 \text{ \AA}$  and  $4 \text{ \AA}$ , respectively. As seen in Fig. 4(b), a combination of such NN hops generates motion along the  $c$ -axis. By themselves, NN jumps would generate nearly isotropic hopping.

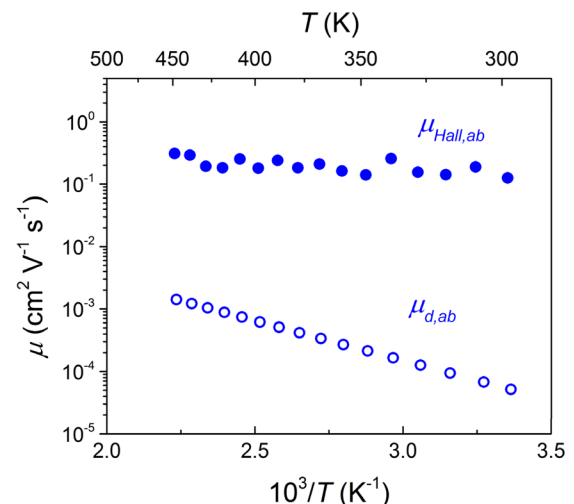


FIG. 3. Hall and deduced-drift mobilities in the  $ab$ -plane are plotted versus reciprocal temperature.

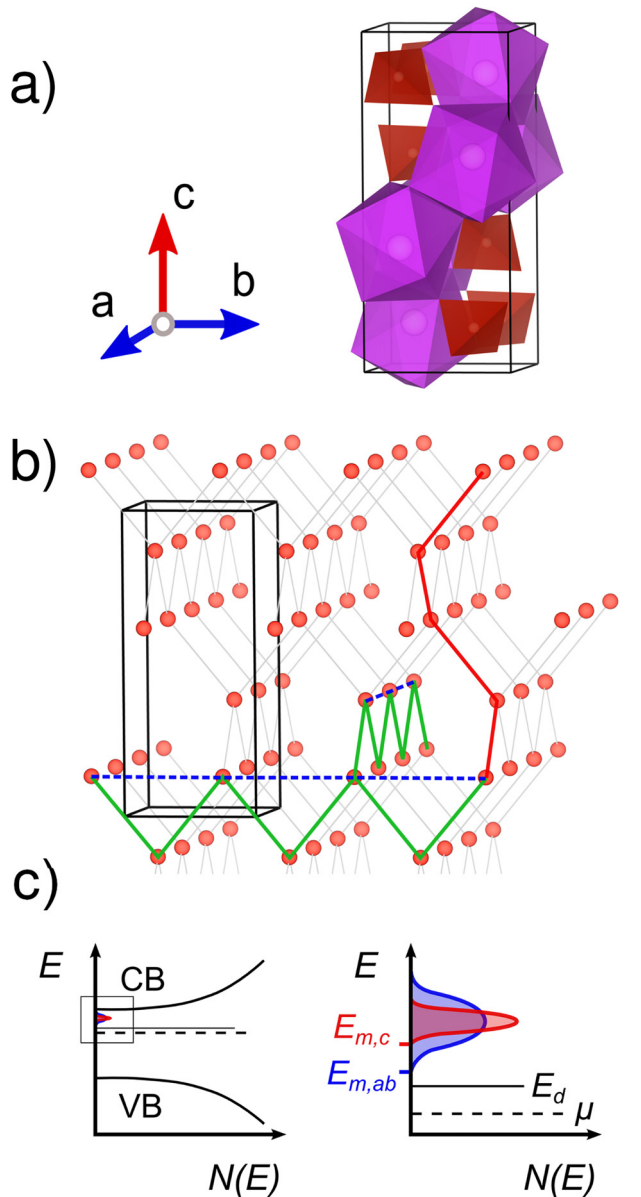


FIG. 4. (a) Monoclinic BVO unit cell showing  $\text{BiO}_8$  (purple) and  $\text{VO}_4$  units (red) and principal axes created with VESTA software.<sup>24</sup> (b) VESTA rendition of a  $3 \times 2 \times 1$  super-cell illustrating the vanadium atom sub-lattice. NN hopping paths are indicated in  $ab$ -plane and  $c$ -axis with green and red solid lines, respectively. NNN jumps in the  $ab$ -plane are shown with blue dashed lines. (c) Left: the location of small-polaron states. Right: schematic illustration of the anisotropy of the width of the small-polaron band. Symmetrical distributions have been used for simplicity.

However, as depicted by the dashed lines in Fig. 4(b), next-nearest-neighbor (NNN) hops in the  $ab$ -plane ( $\sim 5.2 \text{ \AA}$ ) are only slightly longer than NN hops. By contrast, NNN hops with a significant  $c$ -axis component ( $\sim 6.9 \text{ \AA}$ ) are much longer than NN hops. Therefore, the structure of BVO appears to support anisotropic hopping transport. For example, such anisotropic transport would result if  $c$ -axis motion is dominated by NN hopping, while  $ab$ -plane transport is a convolution of NN and NNN jumps. Alternatively stated, the band of small-polaron states is anisotropic with it being wider for motion in the  $ab$ -plane than along the  $c$ -axis (Fig. 4(c)).

An anisotropic small-polaron conduction band that is populated by thermally exciting electrons from lower-lying

donor states of energy  $E_d$  is akin to that of a conventional semiconductor. The position of the chemical potential  $\mu$  is then determined from the requirement that the number of holes in the donor band equals the number of small-polarons in the conduction band

$$N_d e^{(E_d - \mu)/\kappa T} = N_{ab}(T) e^{-(E_{m,ab} - \mu)/\kappa T} + N_c(T) e^{-(E_{m,c} - \mu)/\kappa T}, \quad (3)$$

where  $N_d$  denotes the density of donors, while  $N_{ab}(T)$  and  $N_c(T)$  represent the densities of small-polaron states near their minima at energies  $E_{m,ab}$  and  $E_{m,c}$ . The chemical potential is then

$$\begin{aligned} \mu &= \frac{E_{m,ab} + E_d}{2} + \frac{\kappa T}{2} \ln \left[ \frac{N_d}{N_{ab}(T)} \right] \\ &\quad - \frac{\kappa T}{2} \ln \left[ 1 + \frac{N_c(T)}{N_{ab}(T)} e^{-(E_{m,c} - E_{m,ab})/\kappa T} \right] \\ &\cong \frac{E_{m,ab} + E_d}{2} + \frac{\kappa T}{2} \ln \left[ \frac{N_d}{N_{ab}(T)} \right]. \end{aligned} \quad (4)$$

Analogous to  $\sigma = ne\mu_d$ , the anisotropic values of  $\sigma_0$  are the electronic charge  $e$  multiplied by the pre-exponential factors from the thermally activated carrier density and small-polaron mobility. The pre-exponential factors for the densities of carriers in the appropriate transport states for motion in the  $ab$ -plane and in the  $c$ -direction are  $\cong [N_d N_{ab}(T)]^{1/2}$  and  $\cong N_c(T) [N_d / N_{ab}(T)]^{1/2}$ , respectively. Since electronic carriers are usually able to adjust to the relatively slow movements of the solid's atoms, small-polaron hops are generally adiabatic.<sup>7</sup> The corresponding pre-exponential factors of the anisotropic mobilities are then  $eg a^2 \nu_0 / \kappa T$ , where  $a$  denotes the jump distance,  $\nu_0$  represents the characteristic vibration frequency, and  $g$  is a numerical factor associated with the hopping sites' geometrical arrangement. In accord with the results of Table I, the calculated conductivity pre-exponential factors for hopping within the  $ab$ -plane and in the  $c$ -direction are, respectively,  $\sigma_{o,ab} \cong 10 \text{ S cm}^{-1}$  and  $\sigma_{o,c} \cong 5 \text{ S cm}^{-1}$  with  $\nu_0 = 2 \times 10^{13} \text{ Hz}$ , thus hopping is adiabatic. Since the doping level of our W:BVO is quite small (0.3%), our values for  $\sigma_0$  are orders-of-magnitude smaller than those for intrinsic small-polaron hopping,  $10^2 - 10^3 \text{ S cm}^{-1}$ .<sup>7,8</sup>

The Seebeck coefficient is the entropy transported with a charge carrier divided by its charge.<sup>25</sup> In most instances, the transported entropy is just the entropy-of-mixing arising from adding a charge carrier to the relevant transport states. Then, the Seebeck coefficient depends on the carrier density and the density of thermally accessible transport states. Increasing the carrier density (e.g., by raising the temperature) decreases the Seebeck coefficient's magnitude. Conversely, increasing the number of thermally accessible transport states (by raising the temperature) increases the Seebeck coefficient's magnitude. The decrease of the magnitudes of the Seebeck coefficients of Fig. 2 with rising temperature implies the predominance of the former effect, that is, the W donors are partially ionized at room temperature.

The Seebeck coefficient for transport within the  $ab$ -plane and  $c$ -direction just depends on the energies of small-

polaron states associated with transport in these directions,  $E_{ab}$  and  $E_c$ <sup>7,25</sup>

$$S_{ab} = -\frac{\kappa \langle E_{ab} - \mu \rangle_{ab}}{e \kappa T} \quad (5)$$

and

$$S_c = -\frac{\kappa \langle E_c - \mu \rangle_c}{e \kappa T}, \quad (6)$$

where the brackets denote an average over the thermally accessible transport states. Incorporating Eq. (4) into Eqs. (5) and (6), these Seebeck coefficients become

$$S_{ab} \cong -\frac{\kappa}{e} \left\{ \frac{(E_{m,ab} - E_d)/2}{\kappa T} + \frac{1}{2} \ln \left[ \frac{N_{ab}(T)}{N_d} \right] + \frac{\langle E_{ab} - E_{m,ab} \rangle_{ab}}{\kappa T} \right\} \quad (7)$$

and

$$S_c \cong -\frac{\kappa}{e} \left\{ \frac{(E_{m,c} - E_{m,ab}) + (E_{m,ab} - E_d)/2}{\kappa T} + \frac{1}{2} \ln \left[ \frac{N_{ab}(T)}{N_d} \right] + \frac{\langle E_c - E_{m,c} \rangle_c}{\kappa T} \right\}. \quad (8)$$

There are three terms within the curly brackets of both Eqs. (7) and (8). The first term falls with increasing temperature, the second term rises weakly with increasing temperature, and the final term is the nearly temperature-independent “heat-of-transport” constant,  $A$ . The relatively strong temperature dependence of the first term ensures that the magnitude of the Seebeck coefficient falls with increasing temperature. The competition between the first and second terms is responsible for the change in slope observed at  $\sim 400$  K in the  $ab$ -plane (Fig. 2). Furthermore, the first term in the expression for the Seebeck coefficient for motion in the  $c$ -direction, Eq. (8), exceeds that for motion within the  $ab$ -plane, Eq. (7), by the energy difference  $E_{m,c} - E_{m,ab}$ . Twice this energy difference,  $2(0.08 \text{ eV} - 0.05 \text{ eV}) = 0.06 \text{ eV}$ , is compatible with the requirement that the net small-polaron-bandwidth be less than the characteristic phonon energy. The relatively large heat-of-transport constants,  $A_{ab} = 4.3$  and  $A_c = 5.2$ , are also consistent with an anisotropic small-polaron band whose width is less than the phonon energy but greater than or comparable to the thermal energy  $\kappa T$ .<sup>7,8,10</sup> Finally, finding  $A_c > A_{ab}$  implies that the anisotropic small-polaron band is more sharply peaked in the  $c$ -direction than in the  $ab$ -plane<sup>10</sup> (Fig. 4(c)).

The customary drift mobility is defined as a carrier’s drift velocity per unit applied electric field. For high-temperature adiabatic small-polaron hopping, this mobility is the product of the pre-exponential factor given above,  $ega^2\nu_0/\kappa T$  ( $\sim 1 \text{ cm}^2 \text{ V}^{-1} \text{ s}^{-1}$  at 300 K) and an Arrhenius factor  $\exp(-E_a/\kappa T)$ , where the mobility activation energy,  $E_a$  is usually greater than  $h\nu_0$ . The mobility activation energies are the differences between  $E_\sigma$  and  $E_S$  in the  $ab$ -plane and  $c$ -direction. Semiclassical small-polaron hopping is implied since these energy differences (250 meV and 220 meV, respectively) greatly exceed the characteristic phonon energy (on the order of 0.1 eV). For motion in the  $ab$ -plane, the drift mobility at 300 K is about  $5 \times 10^{-5} \text{ cm}^2 \text{ V}^{-1} \text{ s}^{-1}$ .

This value is consistent with that inferred from time-resolved microwave conductivity (TRMC) measurements,  $\sim 10^{-4} \text{ cm}^2 \text{ V}^{-1} \text{ s}^{-1}$  at 300 K.<sup>5</sup> The larger mobility activation energy in the  $ab$ -plane is in accord with slightly longer NNN transfers, as  $E_a$  increases with the length of the hop [for example, cf. Fig. 11.4 of Ref. 7].

The Hall mobility is defined as the angle per unit applied magnetic field that a drifting carrier is deflected by this field’s application. For free carriers, the drift and Hall mobilities equal one another. However, for small-polaron hopping the activation energy of the Hall mobility is  $< E_a/3$ .<sup>7,26–28</sup> As a result, a small-polaron’s Hall mobility is generally much larger and much less temperature dependent than its drift mobility. The data of Fig. 3 show that the Hall mobility we measure for our W:BVO is consistent with small-polaron hopping.

In summary, we have reported electronic transport measurements of W:BVO single crystals and established that electrons in this material form small polarons. The anisotropic transport was reconciled by including NNN transfers, which foster enhanced hopping in the  $ab$ -plane. Based on our findings, the low electrical conductivity which limits the utility of W:BVO as a photo-anode for water splitting results from the very low thermally activated mobility intrinsic to small polarons. However, knowing that the carriers are small polarons suggests a means of circumventing this deficiency. In particular, a small-polaron generally exhibits a broad absorption band centered near  $\sim 4E_a$ , about 1 eV for BVO.<sup>7,29</sup> For BVO, this small-polaron absorption band lies well below the strong intrinsic inter-band absorption that begins at 2.5 eV. Significantly, small-polarons’ absorptions produce small-polaron hops [cf. Fig. 9.3 of Ref. 7]. Thus, sub-bandgap illumination of a W:BVO photo-anode should increase its electrical conductivity. This optical remedy for the low dark conductivity of W:BVO exploits its carriers being small polarons.

The authors gratefully acknowledge the U.S. Department of Energy (DOE) Grant No. DE-FG02-09ER16119 and Welch Foundation Grant F-1436. A.J.E.R. acknowledges the Hemphill-Gilmore Endowed Fellowship for financial support. J.S.Z. was supported by NSF MIRT DMR 1122603. We are indebted to C. Capan, L. Zhang, X. Chen, and D. Young for useful discussions on data analysis and Seebeck coefficient measurements. We thank D. Eisenberg for assistance with phase sensitive interferometry to determine sample dimensions.

<sup>1</sup>T. W. Kim and K.-S. Choi, *Science* **343**, 990 (2014).

<sup>2</sup>F. F. Abdi, L. Han, A. H. M. Smets, M. Zeman, B. Dam, and R. van de Krol, *Nat. Commun.* **4**, 2195 (2013).

<sup>3</sup>S. P. Berglund, A. J. E. Rettie, S. Hoang, and C. B. Mullins, *Phys. Chem. Chem. Phys.* **14**, 7065 (2012).

<sup>4</sup>A. J. E. Rettie, H. C. Lee, L. G. Marshall, J.-F. Lin, C. Capan, J. Lindemuth, J. S. McCloy, J. Zhou, A. J. Bard, and C. B. Mullins, *J. Am. Chem. Soc.* **135**, 11389 (2013).

<sup>5</sup>F. F. Abdi, T. J. Savenije, M. M. May, B. Dam, and R. van de Krol, *J. Phys. Chem. Lett.* **4**, 2752 (2013).

<sup>6</sup>H. S. Park, K. E. Kweon, H. Ye, E. Paek, G. S. Hwang, and A. J. Bard, *J. Phys. Chem. C* **115**, 17870 (2011).

<sup>7</sup>D. Emin, *Polarons*, 1st ed. (Cambridge University Press, New York, 2013).

<sup>8</sup>D. Emin, C. Seager, and R. K. Quinn, *Phys. Rev. Lett.* **28**, 813 (1972).

<sup>9</sup>M. Sayer and A. Mansingh, *J. Non-Cryst. Solids* **58**, 91 (1983).

<sup>10</sup>S. A. Baily and D. Emin, *Phys. Rev. B* **73**, 165211 (2006).

<sup>11</sup>A. Bosman and H. Van Daal, *Adv. Phys.* **19**, 1 (1970).

- <sup>12</sup>P. Nagels, *The Hall Effect and Its Applications* (Springer, 1980), p. 253.
- <sup>13</sup>M. Jaime, H. Hardner, M. Salamon, M. Rubinstein, P. Dorsey, and D. Emin, *Phys. Rev. Lett.* **78**, 951 (1997).
- <sup>14</sup>B. Zhao, T. C. Kaspar, T. C. Droubay, J. McCloy, M. E. Bowden, V. Shutthanandan, S. M. Heald, and S. A. Chambers, *Phys. Rev. B* **84**, 245325 (2011).
- <sup>15</sup>K.-H. Yoo, D. Ha, J.-O. Lee, J. Park, J. Kim, J. Kim, H.-Y. Lee, T. Kawai, and H. Y. Choi, *Phys. Rev. Lett.* **87**, 198102 (2001).
- <sup>16</sup>S. S. Alexandre, E. Artacho, J. M. Soler, and H. Chacham, *Phys. Rev. Lett.* **91**, 108105 (2003).
- <sup>17</sup>D. Venkateshvaran, M. Nikolka, A. Sadhanala, V. Lemaury, M. Zelazny, M. Kepa, M. Hurhangee, A. J. Kronemeijer, V. Pecunia, I. Nasrallah, I. Romanov, K. Broch, I. McCulloch, D. Emin, Y. Olivier, J. Cornil, D. Beljonne, and H. Sirringhaus, *Nature* **515**, 384 (2014).
- <sup>18</sup>See supplementary material at <http://dx.doi.org/10.1063/1.4905786> for experimental details, calculation of geometrical factors, and a full description of the data analysis.
- <sup>19</sup>J. Lago, P. Battle, M. Rosseinsky, A. Coldea, and J. Singleton, *J. Phys. Condens. Matter* **15**, 6817 (2003).
- <sup>20</sup>A. W. Sleight, H. Y. Chen, A. Ferretti, and D. E. Cox, *Mater. Res. Bull.* **14**, 1571 (1979).
- <sup>21</sup>A. W. Sleight, K. Aykan, and D. B. Rogers, *J. Solid State Chem.* **13**, 231 (1975).
- <sup>22</sup>A. Walsh, Y. Yan, M. N. Huda, M. M. Al-Jassim, and S.-H. Wei, *Chem. Mater.* **21**, 547 (2009).
- <sup>23</sup>K. E. Kweon, G. S. Hwang, J. Kim, S. Kim, and S. Kim, *Phys. Chem. Chem. Phys.* **17**, 256 (2014).
- <sup>24</sup>K. Momma and F. Izumi, *J. Appl. Crystallogr.* **44**, 1272 (2011).
- <sup>25</sup>D. Emin, in *Wiley Encyclopedia of Electrical and Electronics Engineering*, edited by J. G. Webster (Wiley, New York, 2002).
- <sup>26</sup>L. Friedman and T. Holstein, *Ann. Phys.* **21**, 494 (1963).
- <sup>27</sup>D. Emin and T. Holstein, *Ann. Phys.* **53**, 439 (1969).
- <sup>28</sup>D. Emin, *Ann. Phys.* **64**, 336 (1971).
- <sup>29</sup>D. Emin, *Phys. Rev. B* **48**, 13691 (1993).